Mutations in *ANKRD11* Cause KBG Syndrome, Characterized by Intellectual Disability, Skeletal Malformations, and Macrodontia

Asli Sirmaci,[1,2] Michail Spiliopoulos,[2] Francesco Brancati,[3,4,5] Eric Powell,[1,2] Duygu Duman,[6] Alex Abrams,[1,2] Guney Bademci,[1,2] Emanuele Agolini,[3] Shengru Guo,[1,2] Berrin Konuk,[6] Asli Kavaz,[6] Susan Blanton,[1,2] Maria Christina Digilio,[7] Bruno Dallapiccola,[7] Juan Young,[1,2] Stephan Zuchner,[1,2] and Mustafa Tekin[1,2,6,*]

KBG syndrome is characterized by intellectual disability associated with macrodontia of the upper central incisors as well as distinct craniofacial findings, short stature, and skeletal anomalies. Although believed to be genetic in origin, the specific underlying defect is unknown. Through whole-exome sequencing, we identified deleterious heterozygous mutations in ANKRD11 encoding ankyrin repeat domain 11, also known as ankyrin repeat-containing cofactor 1. A splice-site mutation, c.7570-1G>C (p.Glu2524_Lys2525del), cosegregated with the disease in a family with three affected members, whereas in a simplex case a de novo truncating mutation, c.2305delT (p.Ser769GlnfsX8), was detected. Sanger sequencing revealed additional de novo truncating *ANKRD11* mutations in three other simplex cases. ANKRD11 is known to interact with nuclear receptor complexes to modify transcriptional activation. We demonstrated that ANKRD11 localizes mainly to the nuclei of neurons and accumulates in discrete inclusions when neurons are depolarized, suggesting that it plays a role in neural plasticity. Our results demonstrate that mutations in *ANKRD11* cause KBG syndrome and outline a fundamental role of ANKRD11 in craniofacial, dental, skeletal, and central nervous system development and function.

First described in 1975, the KBG syndrome (MIM 148550) is characterized by macrodontia of the upper central incisors, distinctive craniofacial findings, short stature, skeletal anomalies, and neurological involvement that includes global developmental delay, seizures, and intellectual disability.[1–4] The etiology is unknown. The initial description included seven affected patients from three unrelated families.[4] This condition was named KBG syndrome on the basis of the initials of affected families' surnames. Transmission from male to male was observed in two families, suggesting autosomal-dominant inheritance.[4,5] Since its initial description, KBG syndrome has been described in 59 patients in the literature; most of these cases were simplex, and more males than females were described. (Table S1, available online). It is likely that KBG syndrome is underdiagnosed because many of its features, including intellectual disability, are mild, and none of the features is a prerequisite for the diagnosis. The presence of wide upper central incisors (macrodontia), manifesting after the eruption of the permanent maxillary incisor teeth, is distinctive although not a sufficient sign for diagnosis.[6,7] On the basis of a review of 46 cases, it has been suggested that four out of eight major criteria, namely macrodontia, characteristic facial appearance, neurological involvement, delayed bone age, short stature, hand findings, costovertebral anomalies, and the presence of a first-degree relative with the syndrome, be present for the diagnosis.[3]

We ascertained ten families who were from Turkey and Italy whose cases had been published previously[1,5] or who showed a close resemblance to previously described patients with KBG syndrome (Table 1, Figure 1, and Table S1). All patients were evaluated by experienced clinical geneticists to exclude other syndromic forms of intellectual disability. Results of chromosomal studies were normal in each affected individual. This study was approved by the institutional review board at the University of Miami and all participating individuals provided written informed consent. Peripheral blood samples were obtained for DNA and RNA extraction.

Family 1 included a previously published affected father and his two affected sons.[5] DNA samples of the affected father and one affected son (individuals I-1 and II-2 in family 1; Figure 1) and a simplex case (individual 1 in family 2) were screened with whole-exome capture followed by next-generation sequencing. Roche EZ Exome v2.0 kit was used for extracting the target regions from genomic libraries for exome sequencing. Each captured sample was run on two lanes of an Illumina GAIIx platform, which allows 75 bp paired-end reads. Raw data were analyzed with v1.7 of the Illumina analysis pipeline. Sequence reads were aligned to reference human genome with the Mapping and Assembly with Quality (MAQ) software v0.7.1. Variant calls were also made with MAQ and annotated with SeattleSeq into functional categories such as missense, nonsense, splice sites, coding, noncoding,

[1]John P. Hussman Institute for Human Genomics, University of Miami Miller School of Medicine, Miami, FL 33136, USA; [2]Dr. John T. Macdonald Department of Human Genetics, University of Miami Miller School of Medicine, Miami, FL 33136, USA; [3]Istituto di Ricovero e Cura a Carattere Scientifico (IRCCS) Casa Sollievo della Sofferenza, San Giovanni Rotondo, Mendel Laboratory, 00198 Rome, Italy; [4]Department of Biopathology and Diagnostic Imaging, Tor Vergata University, 00133 Rome, Italy; [5]Department of Biomedical Sciences, d'Annunzio University, 66100 Chieti, Italy; [6]Division of Pediatric Genetics, Ankara University School of Medicine, 06100 Ankara, Turkey; [7]IRCCS Bambino Gesù Children Hospital, 00198 Rome, Italy
*Correspondence: mtekin@med.miami.edu
DOI 10.1016/j.ajhg.2011.06.007.

Table 1. Phenotypic Findings and Identified *ANKRD11* Mutations in Study Subjects

	Family 1			Family 2	Family 3	Family 4	Family 5
KBG SYNDROME	**II-1**[a]	**II-2**[a]	**I-1**[a]	**Individual 1**	**Individual 1**	**Individual 1**[b]	**Individual 1**
ANKRD11 mutation (heterozygous)	c.7570-1G>C (p.Glu2524_Lys2525del)			c.2305delT (p.Ser769GlnfsX8)	c.7189C>T (p.Gln2397X)	c.5953_5954delCA (p.Gln1985GlufsX46)	c.6071_6084delCGT ACGCTCTGCCC (p.Pro2024ArgfsX3)
Country of origin	Turkey			Turkey	Turkey	Italy	Italy
Sex	M	M	M	M	M	M	M
Macrodontia[c]	+	+	+	+	+	+	not applicaple
Craniofacial findings	low anterior and posterior hairlines, brachycephaly, triangular face, synophrys, long palpebral fissures, hypertelorism, ptosis, prominent nasal bridge, anteverted nostrils, long philtrum, large and prominent ears			triangular face with pointed chin, low anterior hairline, long palpebral fissures, ptosis, anteverted nostrils, long philtrum, prominent ears	prominent forehead, brachycephaly, triangular face, synophrys, long palpebral fissures, hypertelorism, anteverted nostrils, posteriorly rotated ears, long philtrum, short and webbed neck	low anterior and posterior hairlines, triangular face, ptosis, hypertelorism, prominent nasal bridge, anteverted nostrils, long philtrum, large and prominent ears, short and webbed neck	low anterior and posterior hairlines, triangular face with pointed chin, synophrys, long and downslanting palpebral fissures, ptosis, hypertelorism, prominent nasal bridge, anteverted nostrils, long philtrum, tented upper lip, prominent ears
Hand findings	short hands with clinodactyly of the 5th fingers and ulnar deviation of the 2nd fingers			short hands with clinodactyly of the 5th fingers and ulnar deviation of the 2nd fingers, cutaneous syndactyly of fingers and toes	short hands with clinodactyly of the 5th fingers	short hands with clinodactyly of the 5th fingers, cutaneous syndactyly of fingers and toes	short hands with clinodactyly of the 5th fingers and ulnar deviation of the 2nd fingers
Short stature	+	+	+	+	−	+	+
Neurological involvement	seizures, mild- moderate ID	seizures, mild-moderate ID, ADHD	moderate ID	mild ID	history of developmental delay, moderate ID	moderate ID with hyperactivity, anxiety, and poor concentration	moderate ID
Delayed bone age	+	+	NA	+	NA	NA	+
Costovertebral anomalies	accessory cervical ribs	CSB	thoracic kyphosis, CSB	accessory cervical ribs	−	accessory cervical ribs	−
First-degree relative with KBG	+	+	+	−	−	−	−
Others	cryptorchidism	cryptorchidism, mild SNHL	cryptorchidism, epispadias	cryptorchidism	cryptorchidism	−	cryptorchidism

[a] Previously published.[5]
[b] Previously published.[1]
[c] Permanent central incisor size is ≥10 mm in males and ≥9.7 mm in females. The following abbreviations are used: NA, not available; ID, intellectual disability; ADHD, attention deficit hyperactivity disorder; CSB, closed spina bifida; SNHL, sensorineural hearing loss.

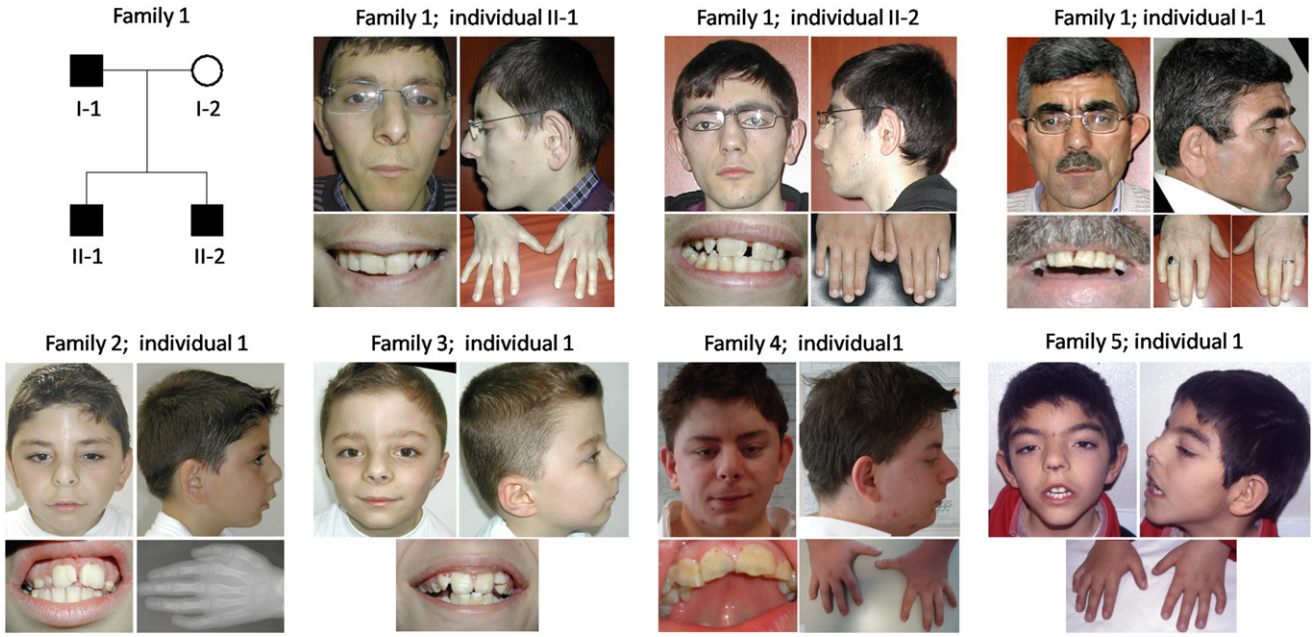

Figure 1. Phenotypic Features of KBG Syndrome
Written consents were obtained from all participants for publication of clinical images. Distinct facial features of KBG syndrome include a triangular face, low anterior and posterior hairlines, synophrys, hypertelorism, eyelid ptosis, a broad and high nasal bridge, an upturned nose, a long philtrum, and wide permanent central incisors (≥10 mm in males and ≥9.7 mm in females). Hand anomalies include brachydactyly, clinodactyly, and cutaneous syndactyly. Photographs were taken when individuals in family 1 were 25 years old (II-1), 22 years old (II-2), and 46 years old (I-1) and individual 1 in family 2 was 9 years old. Facial and dental pictures were taken when individual 1 in family 3 was 6 and 11 years old, respectively. Individual 1 in family 4 was 21 years old and individual 1 in family 5 was 9 years old when photographs were taken.

and untranslated regions. A total average of 10.2 Gb of sequence (67,930,230 pairs of reads) aligned to the exome target for the samples. An average depth of 125× and 95% (>5×) coverage of the targeted-exome region were obtained for each sample (Table S2).

DNA variants obtained with exome sequencing were filtered on the basis of the presence of a variant in the same gene in all three tested individuals. Only 11 genes had variants that were nonsynonymous, nonsense, splice site, or indel-causing frameshifts and were not present in the dbSNP132 or 1000 Genomes databases (Table 2). We used Sanger sequencing to confirm variants obtained through exome sequencing as well as to evaluate cosegregation of variants with the phenotype. PCR reactions were run in 25 μl volume applying a touch-down protocol and annealing temperatures between 65°C and 57°C. We visualized PCR products on agarose gels, cleaned over Sephadex columns, and applied to BigDye reactions following the manufacturer's recommendations (Applied Biosystems Inc., CA, USA). We used a DNA Sequencer (ABI 3730xl) to detect mutations. Results were visualized with the Sequencher 4.7 software (Gene Codes Corporation, MI, USA). Sanger sequencing of these variants showed that only a single gene, *ANKRD11* (MIM 611192; RefSeq accession numbers NM_013275.4 [mRNA]; NP_037407.4 [protein]), had a variant that cosegregated with the phenotype in family 1 as a dominant trait and another variant that was de novo in family 2 (Table S3). There was a heterozygous variant, c.7570-1G>C (p.Glu2524_Lys2525del), affecting a splice-acceptor site present in all three affected individuals but absent in the unaffected mother in family 1 (Figure 2). The second *ANKRD11* variant was a heterozygous one base-pair deletion, c.2305delT (p.Ser769GlnfsX8), identified in individual 1 of family 2. Both parents were negative for this mutation.

Sanger sequencing of all exons and intron-exon boundaries of *ANKRD11* was then performed in the remaining eight probands. Each PCR primer used for Sanger sequencing (Table S4) was evaluated for homologous sequences in the genome, and primers specific to *ANKRD11* were chosen. For copy-number changes involving *ANKRD11*, 12 ng genomic DNA was used via TaqMan copy-number assays for *ANKRD11* (Hs05397046_cn) (Applied Biosystems Inc., CA, USA). For each reaction, 1 μl copy number variation

Table 2. Overall Results of Exome Sequencing

Filters	Family 1; Individuals I-1 and II-2	Family 2; Individual 1	Both Families
Genes with a variant	12058	15444	2614
Nonsynonymous, nonsense, splice site, and indel variants	4464	5649	264
Not in dbSNP or 1000 genome	249	487	11

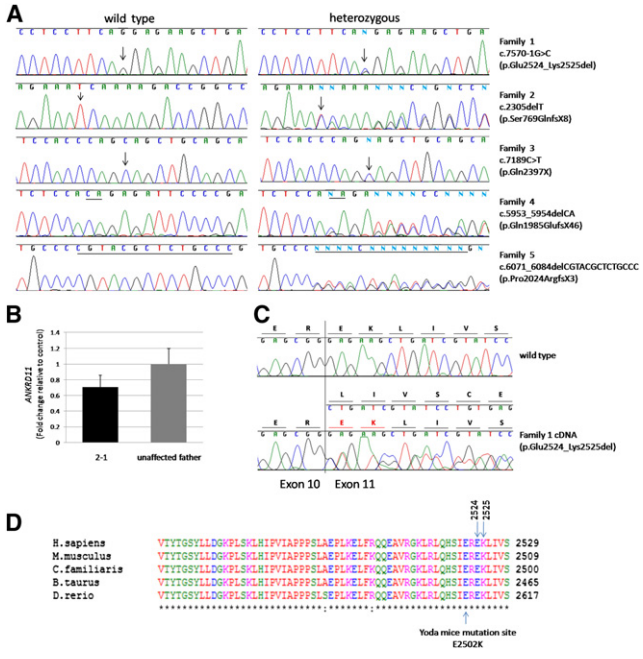

Figure 2. *ANKRD1* Mutations
(A) Sanger results of identified mutations. Affected residues are underlined or indicated with arrows.
(B) Quantitative PCR results of *ANKRD11* in individual 1 of family 2 with a heterozygous c.2305delT mutation (left) and his unaffected father with homozygous wild-type alleles (right).
(C) Sanger sequencing of *ANKRD11* cDNA showing a heterozygous c.7570-1G>C mutation in individual II-1 in family 1. The deleted six base pairs correspond to two amino acids (red).
(D) The alignment of a region from the C-terminal repression domain of ANKRD11 showing the localization of deleted amino acids (E and K) in family 1 as well as the mutation site in Yoda mice.

(CNV) probes (20×, carboxyfluorescein [FAM] labeled), 1 μl RNaseP probe mix (20×, VIC labeled), 10 μl TaqMan Universal PCR Master mix (2×), 1 μl genomic DNA, and 7 μl of water were mixed with a final reaction volume to 20 μl. Reactions were held at 95°C for 10 min, 40 cycles of 95°C for 15 s, and 60°C for 1 min. Samples were run on the ABI7900HT Fast real-time PCR system and analyzed with SDS 2.3 (Applied Biosystems Inc., CA, USA). CopyCaller software was used for analyzing qPCR data with a delta Ct algorithm (Applied Biosystems Inc.,CA, USA). Sanger sequencing revealed heterozygous truncating mutations in three simplex cases in families 3, 4, and 5 (Figure 2). Parents of these patients did not have identified mutations, showing that the mutations were de novo. All five *ANKRD11* mutations were negative in ethnicity-matched controls (Table S5). Sanger sequencing as well as CNV analysis of *ANKRD11* via quantitative PCR remained negative in five other probands. Families 8 and 9 included affected mother and son pairs who were also previously published.[1] Another three families had a single affected individual.

Although the absence of *ANKRD11* mutations in half of our families suggests that KBG syndrome is heterogeneous, we cannot exclude variants in the regulatory regions of the gene. Notably, short stature and cryptorchidism were observed in six of seven patients with an *ANKRD11* mutation,

Figure 3. ANKRD11 Domains and Identified Mutations
The positions of the five identified mutations in ANKRD11 domains. The two mutations identified with exome sequencing are shown with blue characters.

whereas only one out of five without a mutation had short stature, and only one of the four males without an identified *ANKRD11* mutation had cryptorchidism (Table S1).

Four male patients with overlapping de novo microdeletions of 16q24.3, whose common region included *ANKRD11* and an adjacent gene, *ZNF778*, have recently been reported.[8,9] The clinical phenotype included dysmorphic facial features with prominent forehead, arched eyebrows, large ears, and a pointed chin. Recently, another patient who has similar phenotypic features but in whom only the 3′ end of *ANKRD11* is deleted has been reported.[10] All patients had been identified because they had autism spectrum disorder (ASD) and had a mild to moderate degree of intellectual disability. Other variable features included congenital heart defects, disorders of neuronal migration, seizures, cryptorchidism, and kyphoscoliosis. No information on dental abnormalities was available. Facial features of these patients resemble those of patients with KBG syndrome. None of our patients were formally diagnosed with ASD, although it has been reported in patients with KBG syndrome[11].

ANKRD11 encodes ankyrin repeat domain 11, which is also known as ankyrin repeat-containing cofactor 1 (ANCO-1). Ankyrin repeat-containing cofactors are known to interact with the p160 coactivator and nuclear receptor complex by recruiting histone deacetylases in order to inhibit ligand-dependent transcriptional activation.[12] ANKRD11 contains two transcriptional repression domains located at the N and C terminals and an activation domain capable of stimulating transcription[13] (Figure 3). Sanger sequencing of *ANKRD11* cDNA obtained from the peripheral blood of affected individuals in family 1 showed that the splice-site mutation, c.7570-1G>C, leads to an in-frame deletion of six base pairs that results in a loss of two amino acids, p.Glu2524_Lys2525del (Figure 2C). These two amino acids are located in the highly conserved C-terminal repression domain of ANKRD11 (Figure 2D). All five *ANKRD11* mutations identified in this study are predicted to affect this domain of the protein. However, four mutations are predicted to introduce premature termination codons, which could trigger nonsense-mediated mRNA decay and lead to haploinsufficiency of ANKRD11. Nonsense-mediated decay is more likely to be triggered by mutations closer to the 5′end of the gene. We used real-time PCR to quantify *ANKRD11* expression in peripheral blood in individual 1 in family 2; he had a heterozygous

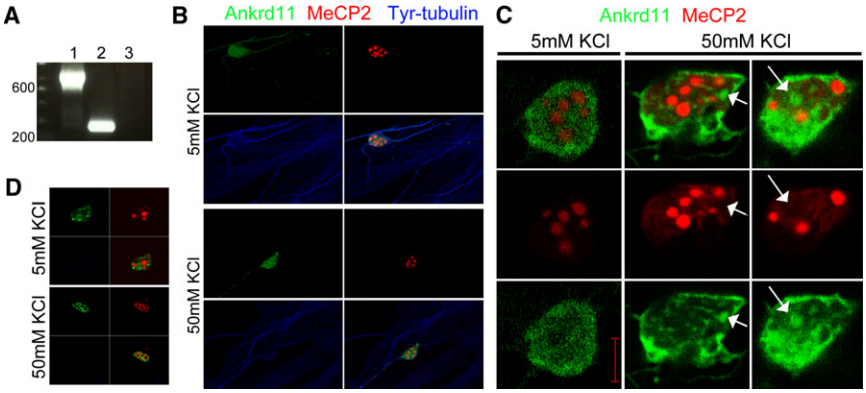

Figure 4. Activity-Dependent Nuclear Aggregation of ANKRD11

(A) RT-PCR expression analysis of *ANKRD11* in adult human brain cDNA. (1) DNA control sample, (2) cDNA sample with reverse transcriptase, and (3) cDNA sample without reverse transcriptase in RT reaction.

(B) Representative image of neonatal cortical neurons transfected with GFP-ANKRD11 along with DsRed-MECP2. Postnatal day 1 neurons (cultured in vitro for 5 days) were cotransfected with GFP-ANKRD11 and Ds-Red-MECP2. Twenty-four hours after transfection, 50 mM KCl (or 5mM to controls plates) was added to the culture media for 90 min, cells were fixed, stained with antibodies to tyrosinated tubulin (blue), and imaged on a confocal microscope.

(C) Higher magnification image of cotransfected neurons to observe GFP-ANKRD11 nuclear inclusions (arrows). GFP-ANKRD11 (green) and DsRed-MeCP2 (red) nuclear aggregates do not colocalize.

(D) Representative glial cells (identified by their lack of tyrosinated-tubulin staining) from the same cultures as in (B). Note that in glial cells, ANKRD11 nuclear inclusions form regardless of KCl addition.

c.2305delT mutation, which was the closest mutation to the 5′ end of ANKRD11. Total RNA was extracted from peripheral blood with a PAXgene blood RNA extraction kit (QIAGEN, CA, USA), and cDNA synthesis from 1 μg of total RNA was performed with a First Strand cDNA Synthesis kit (Roche, SW). For each TaqMan reaction, 40 ng cDNA was mixed with TaqMan Universal PCR Master Mix (Applied Biosystems Inc., CA, USA), B-actin (VIC labeled) and *ANKRD11* (Hs00203193_m1*-FAM labeled) probes. PCR conditions were 50°C for 2 min, 95°C for 10 min, 40 cycles of 95°C for 15 s, and 60°C for 1 min. Data were analyzed by SDS 2.3 and RQ manager 1.2 (Applied Biosystems Inc., CA, USA) software. Results showed that *ANKRD11* expression in individual 1 in family 2 was reduced compared to the expression observed in his unaffected father; this difference suggests that nonsense-mediated mRNA decay was triggered (Figure 2B). However, Sanger sequencing of *ANKRD11* cDNA in individual 1 in family 2 demonstrated the mutant allele, indicating that the mRNA decay is not complete (Figure S1).

Yoda mice are heterozygous for an *Ankrd11* missense mutation, which is only one amino acid away from the two amino acids deleted by the splice-site mutation in family 1 (Figure 2D). They present with craniofacial anomalies that include deformed nasal bones, shortened snouts, and wider skulls[14] and are similar to the craniofacial anomalies seen in KBG syndrome. Kyphoscoliosis, as well as reduced bone mineral density, develop with age in Yoda mice but no other costovertebral anomalies or macrodontia were reported. The oldest patient in our study was 46 years old (individual I-1 in family 1), had a heterozygous p.Glu2524_Lys2525del mutation, and developed moderate kyphosis and osteopenia (his T-score was −1.6 at L1–L4) with age. It is interesting to note the presence of typical phenotypic features in both patients and in Yoda mice with mutations affecting only the C-terminal repression domain of ANKRD11. Although these mutations could conceivably destabilize the entire protein, it is possible that the impaired function of this domain is sufficient to produce the KBG phenotype.

Little is known about the putative brain-related function of ANKRD11. Data available from the Human Protein Atlas (ENSG00000167522) suggest that ANKRD11 is expressed in the brain at comparatively high levels. To start investigating the functional role of ANKRD11 in the central nervous system, we first confirmed that it was expressed in the human brain via nonquantitative RT-PCR analysis by using *ANKRD11* specific primers and an adult human brain cDNA library (Figure 4A). ANKRD11 has been shown to form nuclear inclusions in nonneuronal cell lines.[12] Therefore, to determine the subcellular localization of ANKRD11 in brain cells, we transfected a GFP-tagged version of ANKRD11 into mouse neonatal cerebral cortical primary cultures. Primary cortical tissue was dissected from 129/SvEv mouse embryos at postnatal day 1 and cultured as previously described.[15] Dissociated cells were plated onto poly-d-lysine-coated coverslips on 6-well dishes at a density of 150,000–200,000/cm^2. Cells were maintained in a neurobasal medium (Invitrogen) with B27 serum-free supplements (Invitrogen), L-glutamine (0.5 mM), and penicillin/streptomycin (1%). After 5 days, cultures were transfected with full-length *ANKRD11* fused to GFP (GFP-ANKRD11, generously provided by Paul Nielsen, Hanson Institute, Adelaide, Australia) and DsRed-MeCP2 with a standard calcium phosphate precipitation protocol.[16] Twenty-four hours after transfection, cultures were treated with 50 mM KCl for 24 hr. Transfected cells were identified by GFP/DsRed expression under confocal fluorescence microscopy (LSM 710 Laser Scanning Microscope, Zeiss). We observed that the GFP-ANKRD11 localizes mainly to the nuclei of neurons (Figure 4B) and glial cells (Figure 4D), and only a relatively small amount is localized in the cytoplasm (data not shown). Epigenetic processes such as modification of histone acetylation have been implicated in the changes in gene expression that occur during neural plasticity. Because it has been reported that ANKRD11

can recruit histone acetyltransferases[10] and deacetylases[9] and can interact with the p160 coactivator family, we examined whether membrane depolarization affected ANKRD11 subcellular location. Under resting conditions, ANKRD11 was highly enriched in the nucleus and had a homogeneously diffused distribution (Figures 4B and 4C). Depolarizing the cells with 50 mM KCl significantly induced nuclear accumulation of ANKRD11 in discrete inclusions (Figures 4B and 4C). MeCP2, a transcriptional regulator also linked to intellectual disability, interacts with histone-modifying enzymes, is sensitive to neuronal activity, and accumulates in heterochromatic puncta. Cotransfection of GFP-ANKRD11 and DsRed-MeCP2 into embryonic cortical cultures showed that the activity-enhanced ANKRD11-containing inclusions are not co-occupied by MeCP2, suggesting that these proteins might regulate expression of two distinct sets of genes. These data suggest that ANKRD11 might participate in the regulation of cellular mechanisms that underlie activity-dependent plasticity.

In conclusion, our results indicate that *ANKRD11* mutations are a cause of KBG syndrome and delineate a fundamental role of ANKRD11 in craniofacial, dental, skeletal, and central nervous system development and function. Further studies are warranted to identify other genetic defects of this genetically heterogeneous condition.

Supplemental Data

Supplemental Data include one figure and five tables and can be found with this article online at http://www.cell.com/AJHG/.

Acknowledgments

This study is supported in part by funds from the University of Miami and a grant (Ricerca Corrente 2011) to F.B. and E.A.

Received: May 15, 2011
Revised: June 7, 2011
Accepted: June 10, 2011
Published online: July 21, 2011

Web Resources

The URLs for data presented herein are as follows:

1000 Genomes, http://www.1000genomes.org
dbSNP132 Short Genetic Variations, http://www.ncbi.nlm.nih.gov/snp
Human Protein Atlas, http://www.proteinatlas.org
Online Mendelian Inheritance in Man (OMIM), http://www.omim.org

References

1. Brancati, F., D'Avanzo, M.G., Digilio, M.C., Sarkozy, A., Biondi, M., De Brasi, D., Mingarelli, R., and Dallapiccola, B. (2004). KBG syndrome in a cohort of Italian patients. Am. J. Med. Genet. A. *131*, 144–149.
2. Zollino, M., Battaglia, A., D'Avanzo, M.G., Della Bruna, M.M., Marini, R., Scarano, G., Cappa, M., and Neri, G. (1994). Six additional cases of the KBG syndrome: Clinical reports and outline of the diagnostic criteria. Am. J. Med. Genet. *52*, 302–307.
3. Skjei, K.L., Martin, M.M., and Slavotinek, A.M. (2007). KBG syndrome: Report of twins, neurological characteristics, and delineation of diagnostic criteria. Am. J. Med. Genet. A. *143*, 292–300.
4. Herrmann, J., Pallister, P.D., Tiddy, W., and Opitz, J.M. (1975). The KBG syndrome-a syndrome of short stature, characteristic facies, mental retardation, macrodontia and skeletal anomalies. Birth Defects Orig. Artic. Ser. *11*, 7–18.
5. Tekin, M., Kavaz, A., Berberoğlu, M., Fitoz, S., Ekim, M., Ocal, G., and Akar, N. (2004). The KBG syndrome: Confirmation of autosomal dominant inheritance and further delineation of the phenotype. Am. J. Med. Genet. A. *130A*, 284–287.
6. Dowling, P.A., Fleming, P., Gorlin, R.J., King, M., Nevin, N.C., and McEntagart, M. (2001). The KBG syndrome, characteristic dental findings: A case report. Int. J. Paediatr. Dent. *11*, 131–134.
7. Smithson, S.F., Thompson, E.M., McKinnon, A.G., Smith, I.S., and Winter, R.M. (2000). The KBG syndrome. Clin. Dysmorphol. *9*, 87–91.
8. Marshall, C.R., Noor, A., Vincent, J.B., Lionel, A.C., Feuk, L., Skaug, J., Shago, M., Moessner, R., Pinto, D., Ren, Y., et al. (2008). Structural variation of chromosomes in autism spectrum disorder. Am. J. Hum. Genet. *82*, 477–488.
9. Willemsen, M.H., Fernandez, B.A., Bacino, C.A., Gerkes, E., de Brouwer, A.P., Pfundt, R., Sikkema-Raddatz, B., Scherer, S.W., Marshall, C.R., Potocki, L., et al. (2010). Identification of ANKRD11 and ZNF778 as candidate genes for autism and variable cognitive impairment in the novel 16q24.3 microdeletion syndrome. Eur. J. Hum. Genet. *18*, 429–435.
10. Youngs, E.L., Hellings, J.A., and Butler, M.G. (2011). ANKRD11 gene deletion in a 17-year-old male. Clin. Dysmorphol. *20*, 170–171.
11. Hah, M., Lotspeich, L.J., Phillips, J.M., Torres, A.D., Cleveland, S.C., and Hallmayer, J.F. (2009). Twins with KBG Syndrome and Autism. J. Autism Dev. Disord. *12*, 1744–1746.
12. Zhang, A., Yeung, P.L., Li, C.W., Tsai, S.C., Dinh, G.K., Wu, X., Li, H., and Chen, J.D. (2004). Identification of a novel family of ankyrin repeats containing cofactors for p160 nuclear receptor coactivators. J. Biol. Chem. *279*, 33799–33805.
13. Zhang, A., Li, C.W., and Chen, J.D. (2007). Characterization of transcriptional regulatory domains of ankyrin repeat cofactor-1. Biochem. Biophys. Res. Commun. *358*, 1034–1040.
14. Barbaric, I., Perry, M.J., Dear, T.N., Rodrigues Da Costa, A., Salopek, D., Marusic, A., Hough, T., Wells, S., Hunter, A.J., Cheeseman, M., and Brown, S.D. (2008). An ENU-induced mutation in the Ankrd11 gene results in an osteopenia-like phenotype in the mouse mutant Yoda. Physiol. Genomics *32*, 311–321.
15. Young, J.I., and Zoghbi, H.Y. (2004). X-chromosome inactivation patterns are unbalanced and affect the phenotypic outcome in a mouse model of rett syndrome. Am. J. Hum. Genet. *74*, 511–520.
16. Xia, Z., Dudek, H., Miranti, C.K., and Greenberg, M.E. (1996). Calcium influx via the NMDA receptor induces immediate early gene transcription by a MAP kinase/ERK-dependent mechanism. J. Neurosci. *16*, 5425–5436.